Original Articles

Safety and Characterization of a Novel Multi-channel TMS Stimulator

Yiftach Roth [a,d,*], Yechiel Levkovitz [b,c,1], Gaby S. Pell [a,d], Moria Ankry [d], Abraham Zangen [a,d,*]

[a] Department of Life Sciences, Ben-Gurion University, Beer Sheva, Israel
[b] The Emotion-Cognition Research Center, Shalvata Mental Health Care Center, Hod-Hasharon, Israel[1]
[c] Sackler Faculty of Medicine, Tel Aviv University, Tel Aviv, Israel
[d] Brainsway Ltd, Israel

ABSTRACT

Background: Currently available TMS stimulators have a single channel operating a single coil.
Objective: To outline and present physical and physiological benefits of a novel convenient multi-channel stimulator, comprising five channels, where the stimulation parameters of each channel are independently controllable.
Methods: Simultaneous and sequential operation of various channels was tested in healthy volunteers. Paired pulses schemes with various inter-stimulus intervals (ISIs) were studied for the hand APB and the leg AH muscles. Energy consumption and coil heating rates with simultaneous operation of 4 channels was compared to a single figure-8 coil.
Results: Repetitive operation of separate channels with different stimulation parameters is demonstrated. The operations of various channels can be combined simultaneously or sequentially to induce multiple pulses with ISIs of μs resolution. A universal pattern of inhibition and facilitation as a function of ISI was found, with some dependence on coils configurations and on pulse widths. A strong dependence of the induced inhibition on the relative orientation of the conditioning and test pulses was discovered. The ability of this method to induce inhibition in shallow brain region but not in deeper region, thus focusing the effect in the deep brain region, is demonstrated. A significant saving in energy consumption and a reduction in coil heating were demonstrated for several channels operated simultaneously compared to a standard single channel figure-8 coil.
Conclusions: The multi-channel stimulator enables the synchronized induction of different excitability modulations to different brain regions using different stimulation patterns in various channels. Multiple pulses operation with coils with various depth profiles can increase the focality of TMS effect in deep brain regions.

© 2014 Elsevier Inc. All rights reserved.

Introduction

Over the past 20 years, TMS has proved highly successful in furthering our understanding of the neurophysiology of the brain and in clinical treatment of neuropsychiatric and neurological diseases. The available stimulating devices are relatively simple and have remained largely unchanged since Barker and Jalinous' original device described in the early 1980s [1,2]. A high voltage is rapidly switched and discharged through a capacitor–inductor circuit giving rise to damped sinusoidal current pulses [3]. These systems are relatively inefficient [4–6] since only a small percentage of the pulse energy is transferred to the target brain tissue. In repetitive TMS the high currents lead to considerable coil heating effects that are far from optimal in terms of both hardware and patient safety. Furthermore, the implementation of TMS is commonly limited to the discharge of pulses through a single coil connected to a single stimulator channel placed on the area of interest. The use of different capacitance values [4,7] or of two stimulators connected to a single coil [8] to produce various pulse durations and waveforms was presented in a study and some commercial devices. A recent analytical study [9] suggested that some novel near-triangular current pulse shapes may increase

substantially the efficacy of neural activation. Novel TMS stimulator topologies were suggested and presented recently [10–12] enabling to produce near-triangular current pulses with controllable pulse durations and amplitudes of the two phases. These devices were shown to lead to significant reduction in energy consumption and coil heating. Yet, the ability to "parallelize" TMS with multiple coil elements should greatly expand the scope and improve the efficiency of TMS. The idea of TMS coils designed with multiple stimulation channels was initially described by Ruohonen [13,14]. In that work, a design of an array of relatively small (<5 cm diameter) coils was shown by simulation to enable more focal stimulation. However, this has remained a theoretical concept. Other coil designs with more than a single coil element have been proposed [15–22] with advantages of performance, but none have entered common use. A recent study outlined a method for independent control of the relative polarity of various windings of TMS coils, thus enabling to switch between active and sham modes [23]. In this study, we outline a unique stimulator design with multiple coils each controlled by a dedicated channel. This system allows completely independent control of each coil with flexibility to manipulate any of the host of pulse characteristics, including timing in resolution of μs, amplitude, polarity, frequency and train format. Based on the additive contribution of multiple energy storage sources to the total energy and the reduced required current in each channel, our hypothesis was that connecting several coils (instead of one) to such a design will lead to substantial improvements in hardware, coil heating rate and energy efficiency. Another feature of this novel system is the ability to stimulate simultaneously various brain regions using different stimulation parameters, such as frequency, intensity and pulse width, thus inducing differential physiologic effect in various brain structures. In addition, it is hypothesized that "multi-channel" TMS will foster the development of new strategies to improve a fundamental limitation of conventional clinical TMS, i.e., focality and depth penetration of the stimulating field. For example, by exploiting the timing sensitivity of successive action potentials of a nerve, multiple coils with different field profiles, such as deep TMS H-coils [24–26], can be spatially and temporally coordinated to stimulate preferably at depth. In the present study, a "multi-channel" TMS was constructed and used in order to examine and present such potential benefits.

Methods

Subjects

A total of 34 healthy volunteers (28 men, 6 women) participated in the study (mean age 27). Exclusion criteria were: 1) history of head injury, systemic uncontrolled disease or seizure disorder; 2) pacemaker, metallic implants, or any other contraindication to TMS as specified in the safety guidelines for that procedure [27]; 3) neurophysiological evidence of impairment of central and peripheral nerve conduction. The study protocol was approved by the local Ethical Committee. All subjects gave written informed consent.

Multi-channel stimulator topology

The version of the multi-channel "Multiway" stimulator (Brainsway, Jerusalem, Israel) designed for these initial studies, included five independent channels. Each channel can operate a separate TMS coil. The stimulator circuit topology is shown in Fig. 1.

The control circuit can trigger the gate terminal of each SCR, thus controlling the timing of operation of each channel, in resolution of 1 μs.

Different capacitors are included in the various channels: Capacitors of 180 μF (Channels # 1 and 5), 50 μF (Channels # 3 and 4)

and 25 μF (Channel # 2). This feature allows induction of different pulse widths in the various channels. The maximal capacitor voltage at 100% power output in each channel is 2 kV.

The Multiway stimulator has two principal operation modes:

a. Standard pulses

This mode enables simultaneous operation of two to five channels, where for each channel the stimulation parameters such as stimulator power output, frequency, train duration, inter-train interval and number of trains are controlled independently. As a simple example, a certain coil can be placed over a first brain region and be operated at high frequency (i.e., 10 Hz) by a first channel, while simultaneously a second coil may be placed over a second brain region and operated at low frequency (i.e., 1 Hz) by a second channel.

b. Pulse group

In this mode, pulses from several channels can be combined. The parameters for each channel are controlled independently, including the power output, current polarity and start time in 1 μs accuracy. Pulses from various channels can be initiated either simultaneously or sequentially, with delay times ranging from 0–10 ms in increments of 1 μs. Single and repetitive operation of such pulse groups is available. This mode was used for the paired-pulse experiments described in this study.

TMS coil arrays

The TMS coils and coil arrays used in this study as well as their geometrical and physical features are listed in Table 1.

Inductance and resistance of each coil were measured with LCR meter (Agilent, USA).

Coil arrays are comprised of several independent coils, each connected to a separate Multiway channel.

The 4-Ch Hand Array (4-HA) was designed to be placed with its central segment over the hand motor cortex. The central segment includes windings of all four coils with common direction and current polarity, in order induce optimal combined effect in the hand motor cortex. The coils had to be large enough to induce sufficient field intensity, but not too large in order to allow feasible placement over the head. Hence the 4-HA coil elements have an elliptic shape.

The Double Circular Array (DCA) was also designed to be located over the hand motor cortex. Hence the DCA coils also have an elliptic shape.

The 4-Ch Modulation Array (4-Mod) and the 4 Ch Modulation 90° Array (4-Mod 90°) were designed to be placed both over the hand motor cortex (usually at 45° to the central sulcus) and over the leg motor cortex (usually along the lateral–medial axis). Hence the larger coils of these arrays (C and D in Table 1) have triangular shapes to accommodate comfortable placement over both locations.

All coil arrays were designed with a degree of flexibility to enable good attachment to different head shapes and sizes.

Comparison between stimulators using a standard figure-8 coil

A standard figure-8 coil (Magstim, UK) with internal loop diameters of 7 cm was used to compare between the outputs of a single channel of the Multiway stimulator, channel #1 with a 180 μF capacitor, and a Magstim Rapid[2] stimulator.

The threshold required to reach a motor activation of the left hand abductor policis brevis (APB) with the figure-8-coil was
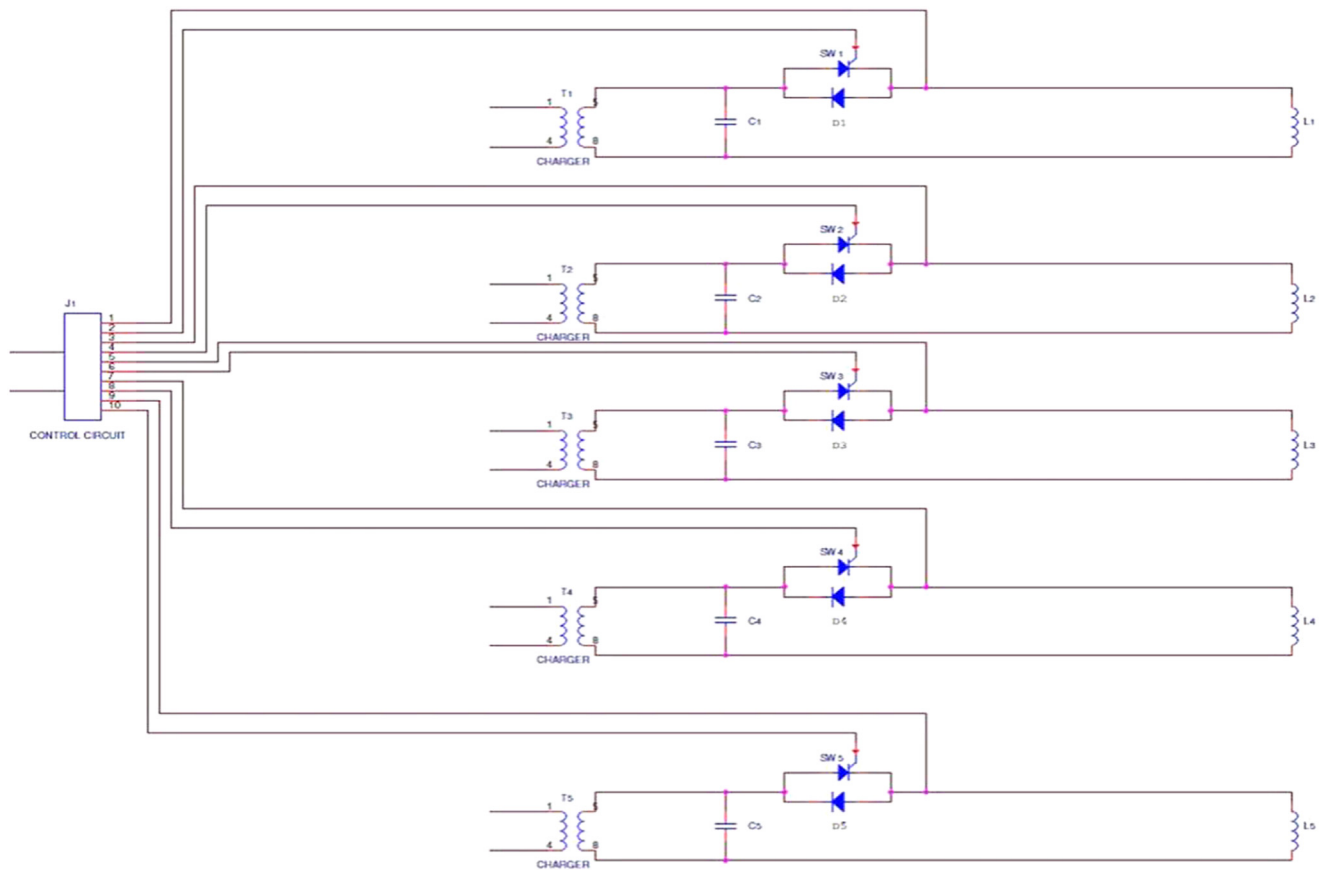
Figure 1. A schematic drawing of the Multiway stimulator comprised of five channels. In each channel a charger circuit charges a capacitor to the desired voltage. The maximal capacitor voltage in each channel is 2 kV. The capacitor is discharged into the TMS coil via a bidirectional switch realized by a silicon controlled rectifier (SCR) and a diode in parallel. Hence a biphasic pulse is induced.

measured when connected to each of the stimulators, for 17 subjects. The motor threshold (MT) was measured using EMG measurements of motor evoked potentials (MEPs) (VikingQuest, Carefusion, USA). Threshold was defined as the stimulator intensity required to elicit MEPs of at least 50 µV in 5 out of 10 trials.

The coil positioning method used in all the experiments is described in the Supplementary material.

Energy comparisons: single channel vs multiple channels

The performance of a standard, single element figure-8 coil (Magstim) was compared to that of a multi-channel coil with 4 circular elements. The threshold stimulator outputs required to reach a motor activation of the left hand APB were measured for the figure-8 coil connected to channel #1 (180 µF capacitor) of the Multiway, representing standard TMS stimulation, and for the 4-Ch Hand Array (*4-HA*), representing potential benefit of the novel Multiway system. Note that the spatial characteristics of the induced electric field are different in the two cases. The goal here was to compare the performance of a single standard coil with that of multiple coils having similar physical properties (i.e. inductance) connected to several channels. The connection scheme of the *4-HA* array was the following: elements C and D were connected to channels # 1 and 5 (180 µF), respectively, and elements A and B were connected to channels # 3 and 4 (50 µF), respectively. The pulses of channels # 3 and 4 lagged behind the pulses of channels 1 and 5 by 100 µs. Due to the capacitance difference, this interval meant that the second phase turning points of the induced trans-

membrane potential (V_m) swing of all the channels were superimposed [28]. This is demonstrated in Fig. 2, where the typical pulse shapes of the coil current, induced electric field and V_m swing are depicted for the two types of channels.

The power outputs required to reach the MT were measured separately for each pair of channels, and the amplitudes ratios were kept constant when searching for the threshold values with the four channels operated together.

The total energy consumption, coil heat dissipation and induced V_m swing were calculated in each case for 21 subjects (see Supplementary material for details and derivations).

Paired pulses modulation with variable intervals and capacitors combinations

The effect of paired pulses at various inter-stimulus intervals (ISIs) on hand motor cortex excitability was measured in 24 subjects. The ISI determination followed the standard definition as the time from the end of one pulse to the onset of the second pulse. The Double Circular Array (*DCA*) coil was used for these experiments. The *DCA* was located such that one side of the circular-like coils is over the right hemisphere hand motor cortex, and the other side is over the contralateral hemisphere. In all cases the first (*conditioning*) pulse was set to 80% of the *hand APB MT* whilst the stimulation strength of the second (*test*) pulse was fixed at a supra-threshold level (120%) relative to the threshold of hand APB. This corresponds to common parameters to achieve short interval cortical

Table 1
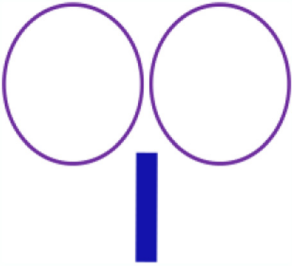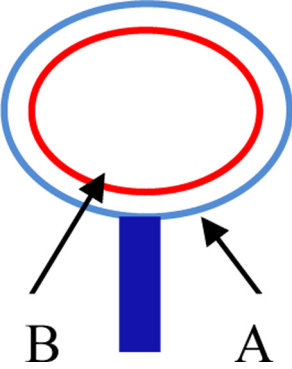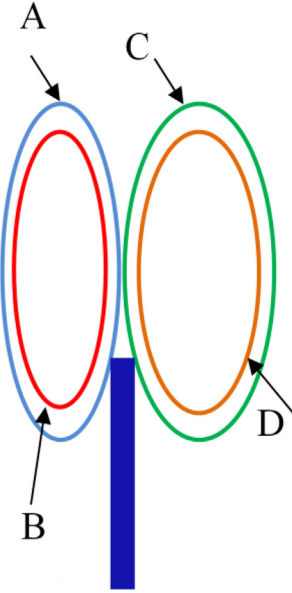TMS coil arrays geometrical and physical features.
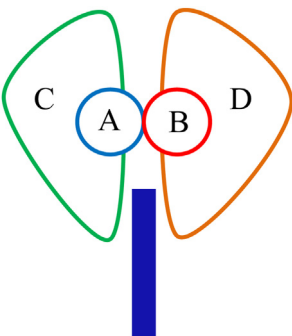
TMS coil arrays geometrical features.

Height [cm]	Width [cm]	Coil element	Schematic drawing	Name of coil array
7 × 2	7 × 2	figure-8 coil		70 mm Double Coil (figure-8)
Inner − 15.5 Outer − 17.5 Inner − 13 Outer − 15	Inner − 17 Outer − 19 Inner − 13.5 Outer − 15.5	A B		Double Circular Array (*DCA*)
Inner − 20 Outer − 23 Inner − 17.5 Outer − 20 Inner − 19 Outer − 21 Inner − 16 Outer − 18	Inner − 7 Outer − 9 Inner − 4.5 Outer − 7 Inner − 14 Outer − 16 Inner − 12 Outer − 14	A B C D		4-Ch Hand Array (*4-HA*)
Inner − 5 Outer − 7 Inner − 5 Outer − 7 Inner − 12 Outer − 17 Inner − 12 Outer − 17	Inner − 5 Outer − 7 Inner − 5 Outer − 7 Inner − 12/7 Outer − 17/12 Inner − 12/7 Outer − 17/12	A B C D		4-Ch Modulation Array (*4-Mod*)

Table 1 (*continued*)

TMS coil arrays geometrical features.				
Height [cm]	Width [cm]	Coil element	Schematic drawing	Name of coil array
Inner − 5	Inner − 5	A		4-Ch Modulation 90° Array (4-Mod 90°)
Outer − 7	Outer − 7			
Inner − 5	Inner − 5	B		
Outer − 7	Outer − 7			
Inner − 12	Inner − 12/7	C		
Outer − 17	Outer − 17/12			
Inner − 12	Inner − 12/7	D		
Outer − 17	Outer − 17/12			

TMS coil arrays physical features				
Inductance [μH]	Resistance [mΩ]	# of windings	Coil element	Name of coil array
16.9 ± 0.3	60 ± 1.0	N/A	figure-8 coil	70 mm Double Coil (figure-8)
15.4 ± 0.3	33 ± 1.0	7	A	Double Circular Array (DCA)
15.9 ± 0.3	32.8 ± 1.0	8	B	
21.3 ± 0.3	44 ± 1.0	10	A	4-Ch Hand Array (4-HA)
21.8 ± 0.3	46 ± 1.0	10	B	
18.0 ± 0.3	41 ± 1.0	10	C	
19.3 ± 0.3	42 ± 1.0	10	D	
14.6 ± 0.3	34.6 ± 1.0	14	A	4-Ch Modulation Array (4-Mod)
14.7 ± 0.3	35.7 ± 1.0	14	B	
15.2 ± 0.3	40.6 ± 1.0	9	C	
15.9 ± 0.3	39.4 ± 1.0	9	D	
15.3 ± 0.3	35.3 ± 1.0	14	A	4-Ch Modulation 90° Array (4-Mod 90°)
14.6 ± 0.3	36.2 ± 1.0	14	B	
14.7 ± 0.3	40.3 ± 1.0	9	C	
15.5 ± 0.3	39.8 ± 1.0	9	D	

inhibition and facilitation [29,30]. The current polarities of the two pulses were the same, and the pulses were biphasic.

Four channel combinations were tested: 180/50, 50/180, 180/180 and 50/50, where the first and second numbers indicate the capacitor type (either 50 or 180 μF) in the channel inducing the conditioning and the test pulse, respectively.

For each capacitors combination, the ISI was varied between 0 and 4500 μs. The following ISIs were used: 0, 100, 200, 300, 400, 500, 600, 700, 800, 900, 1000, 1250, 1500, 1750, 2000, 2250, 2500, 2750, 3000, 3500, 4000 and 4500 μs. The inter-trial interval was at least 5 s. Each ISI was acquired as a block of five conditioned trials, followed by five unconditioned trials, and then five more conditioned trials. The order of ISIs was randomized between blocks. MEP areas from conditioned trials at each ISI and from the unconditioned trials were separately averaged and the ratio between the two calculated. Artefactual EMG readings were rejected from the averaging and the threshold was re-measured when unconditioned trials indicated a change in corticospinal excitability. Results are shown in Table S1 in the Supplementary material. The MEP signal area was measured in each case and the ratio between the conditioned and the unconditioned results was calculated.

Selective inhibition using paired pulses

In order to demonstrate the ability of the Multiway to induce differential excitability modulation in shallow and deeper brain regions, the 4-Ch Modulation Array (4-Mod) was used containing pairs of large and small circular-like coils (see Table 1). The smaller coil pair (A and B in Table 1) possesses a shallower depth profile than the larger pair (C and D in Table 1). In 27 subjects, the smaller coils were connected to channels with 180 μF capacitors and their

stimulation strength was set to 80% of the hand MT whilst the larger coils were connected to channels with 50 μF capacitors and their stimulation strength was fixed at 120% relative to the threshold of chosen target area, either the hand (APB) or the leg (AH, abductor hallucis) muscles. The MEP signal area was measured in each case. In all the experiments described in sections 2.6–2.7 ISIs of 200, 400 and 600 μs were used. In a follow up series of trials, the hand was activated with the conditioning pulse set at 80% of the hand MT while the test pulse was fixed at 120% of the leg. This mimicked the effect induced in superficial structures while activating deep brain structures. The coil orientation for each subject was determined based on the location of the minimal MT. As expected, the optimal orientation over the hand motor cortex was found to be at about 45° to the postero−anterior axis, while over the leg motor cortex it was found to be along the lateral−medial axis.

Effects of coil orientation and cortical target on paired-pulse inhibition

In order to obtain additional insight regarding the inhibition mechanisms, we studied the effect of orientation of the smaller pair of coils inducing the conditioning pulse. The 4 Ch Modulation 90° Array (4-Mod 90°) is identical to the 4-Mod Array, except that the smaller coils A and B are rotated in 90° relative to the larger coils C and D (see Table 1). Hence with the 4-Mod 90° the neural populations affected by the conditioning and the test pulses are likely to be different, since in general neural response depends on the neural structure orientation relative to the electric field orientation.

The 4-Mod 90° and 4-Mod Arrays were compared by paired pulse experiments over hand APB and the leg AH motor cortex locations. In each case, the stimulation strength of the smaller coils
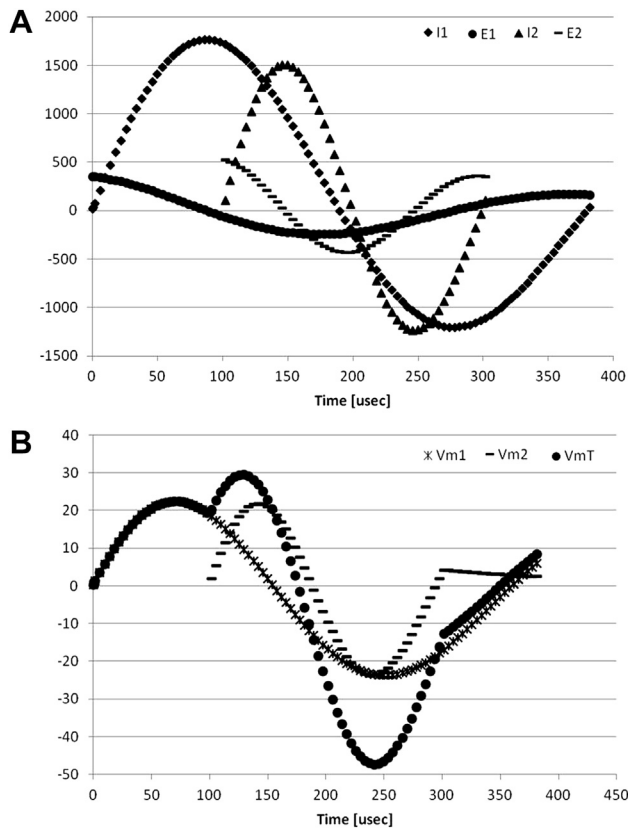
Figure 2. A. Coil currents (I1 and I2) and induced electric fields (E1 and E2) for Multiway channels with capacitors of 180 μF and 50 μF. The pulse of the 50 μF channels starts 100 μs after the pulse of the 180 μF channel. B. Swings in the neural transmembrane potential V_m induced by the two TMS pulses. V_mT indicates the total change in V_m induced by the combination of the two pulses. Note that the minima of the 2nd phase of the two V_m swings coincide.

was set to 80% of the relevant MT whilst the stimulation strength of the larger coils was fixed at 120% of the relevant MT. The coil orientations for each subject were the same as in the experiments described in Section 2.6.

Simultaneous multi-channel operation of repetitive pulses

The ability of the Multiway to produce realistic repetitive operations of several channels with different stimulation parameters was tested. The *4-HA* various coils were connected to various stimulator channels, and several protocols of repetitive operation were programmed and operated. The *4-HA* coils were attached to a head model, and the electric field of each pulse was measured and recorded.

Measurement of electric field

For all the experiments and protocols, the induced electric field pulse characteristics, including amplitude, pulse width and inter-pulse intervals were measured as described previously [13] (see Supplementary material for details).

The depths of stimulation site for the hand APB and leg AH were determined by intersection points of V_m profiles of the small coil pair (A and B in Table 1) and the large coil pair (C and D in Table 1) of the *4-Mod* Array in a method presented previously [31,32] (see Supplementary material for details).

Statistical methods

Paired *t*-tests were used to compare threshold measurements and energy calculations. Measurements that were further than 1.5 times the inter-quartile range (IQR) from the lower and upper quartile points were considered as outliers.

For the paired pulse experiments with the *DCA* coil, a mixed models approach was conducted to explore the impact of the ISI and the capacitor combination on the MEP area in the paired pulse experiments carried out with the *DCA* array. This model was used since not all of the subjects received all of the 4 capacitor combinations and the model is much more tolerant to missing values than the GLM approach. Both ISI and capacitor combination were treated as repeated measures with a covariance type defined by compound symmetry (constant variance and constant correlation). In addition, the capacitor combination was treated as a fixed effect (with a fixed mean over the subjects), while the ISI was defined as a random effect (with inter-individual variation about the mean defined by a variance) for individual slope and intercept values with correlation between them defined by the scaled identity (constant variance, no covariance). A *P*-value of <0.05 was considered as statistically significant. Mean values are quoted together with standard errors (±SE).

A mixed models approach was also conducted to explore the influence of ISI and coil orientation on the MEP area in different cortical areas in the 4 channel array coils. ISI, orientation and cortical target were treated as repeated measures with a covariance type defined by compound symmetry (constant variance and constant correlation). In addition, the ISI, orientation and cortical target were treated as a fixed effect (with a fixed mean over the subjects).

Results

Most of the subjects tolerated well the stimulation sessions. One non-TMS related adverse event was reddening of the nose of one subject. The treating physician confirmed this was due to allergic response from an insect bite. No other adverse events were reported.

Comparison between stimulators using a figure-8 coil

The MTs of the left hand APB were measured in 17 subjects using a figure-8 coil connected to either the Magstim Rapid[2] or channel #1 of the Multiway (Fig. 3). The corresponding stimulator voltages for threshold were very similar (2-sided paired *t*-test, no significant

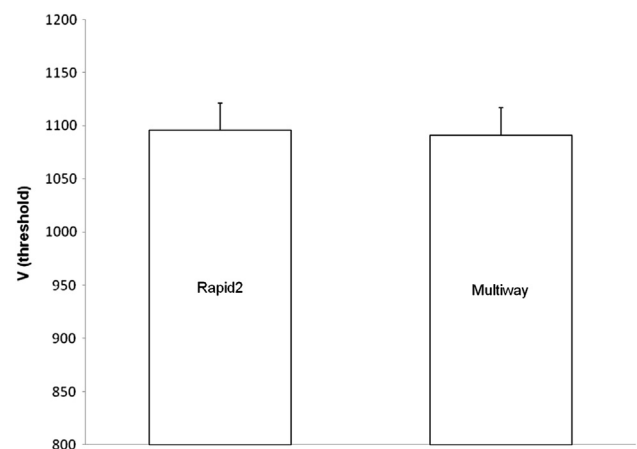**Figure 3.** Comparison of motor thresholds using Magstim Rapid[2] and Multiway stimulators with a figure-8 coil. Shown are means ± SE of stimulator voltage corresponding to motor threshold in the right hand APB muscle of 17 subjects.

Table 2
Summary of results of all the experiments at motor threshold.

	Coil array	Coils/capacitors combination	Pulse width [μs]	MT [%]	E_{thr} [V/m][a]	V_m^{thr} [mV][b]	W_T [J]	Q_T [J]
1	70 mm Double Coil (figure-8)	figure-8 coil − >180	345	55 ± 1	74	19.21	111 ± 5	79 ± 4
2	4-Ch Hand Array (4-HA)	C,D − 180	360	C,D: 20 ± 1	73	18.60	51 ± 2	24 ± 1
		A,B − 50		A,B: 31 ± 1				
3		C − 180	360	C: 37 ± 1	83	20.80	91 ± 7	42 ± 3
		A − 50		A: 61 ± 2				
4		C − 180	360	53 ± 1	58	17.54	111 ± 4	52 ± 2
5	Double Circular Array (DCA)	A − 180	331	48 ± 1	62	18.08	83 ± 3	42 ± 2
6		B − 180	336	39 ± 1	51	14.96	55 ± 3	27 ± 1
7		A − 50	175	80 ± 1	89	15.43	64 ± 2	20 ± 1
8		B − 50	178	67 ± 1	85	15.17	45 ± 1	13.7 ± 0.4
9	4-Ch Modulation Array (4-Mod)	A,B − 180 Hand	355	51 ± 1	64	17.79	187 ± 7	101 ± 4
10		C,D − 50 Hand	180	39 ± 1	106	18.20	30 ± 2	11.0 ± 0.6
11		C − 50 Hand	180	78 ± 1	117	19.66	61 ± 1	22.5 ± 0.6
12		A,B − 180 Leg	355	90 ± 2	67	18.52	583 ± 26	315 ± 14
13		C,D − 50 Leg	180	57 ± 1	112	19.07	65 ± 2	24 ± 1

[a] Measured E at threshold at depth of 2 cm (hand) or 3 cm (leg).
[b] Calculated V_m at threshold at depth of 2 cm (hand) or 3 cm (leg).

difference, $P = 0.72$). This confirms that the Multiway can be used to drive standard single-channel coils with identical performance to a conventional stimulator.

Single channel vs multiple channels: Energy consumption and heat dissipation

Table 2 summarizes the results of all experiments and coils/capacitors combinations at the average threshold for motor activation, including pulse width, stimulator power output in each channel, energy consumption, heat dissipation, the electric field measured in a head model at appropriate depths of hand and leg areas (2 cm hand APB) or 3 cm (leg AH), and the corresponding calculated V_m at these locations.

The depths were determined based on the interception points of the V_m plots for the small and large coil pairs of the 4-Mod Array (Fig. S1 in the Supplementary material). The calculated values were 1.68 ± 0.33 cm and 2.67 ± 0.63 cm for the hand and leg, respectively. The obtained threshold V_m values were very similar (19.5 ± 4.0 mV for the hand; 20.8 ± 6.4 mV for the leg).

As can be seen from Table 2, the threshold V_m seems to be uniform across experiments within 10% variability (17.9 ± 1.8 mV, mean ± SD).

Maps of distribution of electric field and V_m for all coils/capacitors combinations at threshold are shown in Fig. S2 in the Supplementary material. It can be seen that while the electric field values vary significantly between the experiments, the threshold V_m value at the relevant motor cortex site is quiet constant.

The performance of a standard figure-8 coil was compared to that of a multi-channel coil with 4 circular elements (the 4-HA Array, see Table 1) in 21 subjects. Fig. 4A indicates that a substantial reduction in energy consumption of 54% was enabled with use of the 4-channel coil array (51 ± 2 J for the 4-HA Array compared to 111 ± 5 J for the figure-8 coil). The difference between groups was significant ($P < 0.0001$, 2-sided paired t-test).

The results shown in Fig. 4B indicate a reduction of 70% in the energy dissipated as heat with use of the 4-channel coil array (24 ± 1 J for the 4-HA Array compared to 79 ± 4 J for the figure-8 coil). The difference between groups was significant ($P < 0.0001$, 2-sided paired t-test).

From rows 10−11 in Table 2 comparing single or a pair of similar coils connected to channels with the same capacitance, it can be seen that the energy consumption and heat dissipation reduce twofold when using two channels. Comparing lines 2−3 in Table 2

we see 44% reduction in energy and 43% reduction in heat dissipation when using 4 channels compared to 2 channels.

Paired pulses modulation with variable intervals and capacitors combinations

For all capacitor combinations a similar modulation pattern induced by paired pulses was obtained. In Fig. 5 are plotted the averaged ratios of paired pulse/single pulse MEP area obtained from hand APB as a function of ISI for the various capacitor combinations.
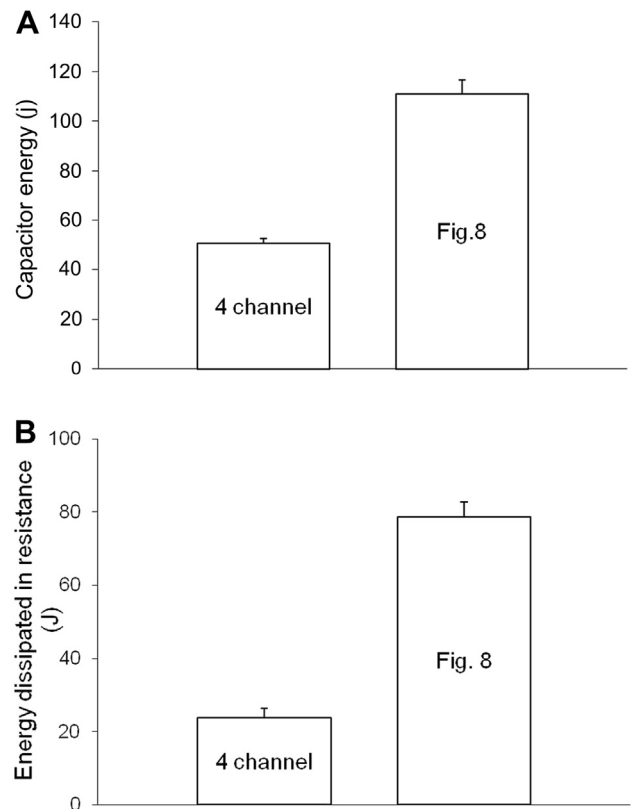

Figure 4. Comparison of energy stored in the stimulator capacitor (A) and of energy dissipated as heat in the coil (B) at threshold for standard single channel and novel 4-channel coil array designs on the Multiway system. Averages over 21 subjects are shown from measurements of motor threshold in the right hand APB muscle.
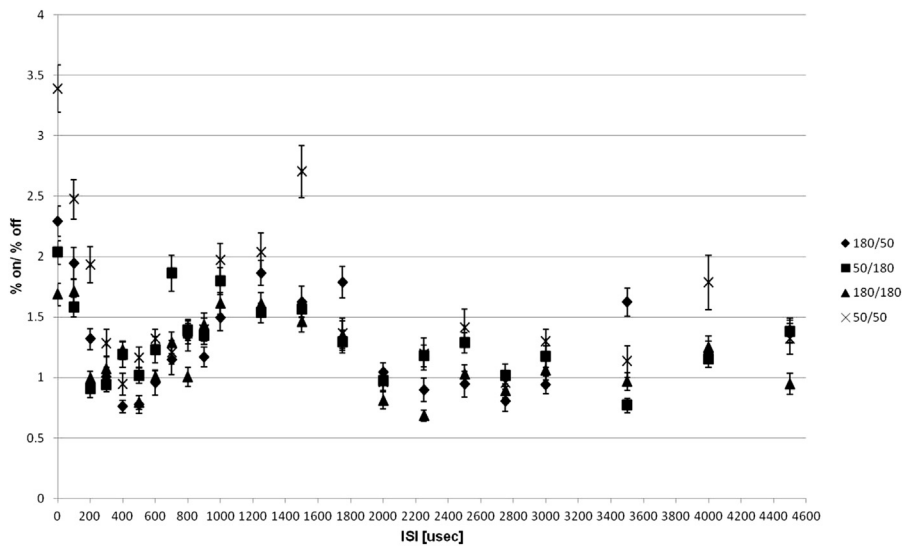
Figure 5. Excitability modulation induced by paired pulses for the hand APB as a function of inter-stimulus interval (ISI), using the *DCA* Array, for 4 capacitor combinations. The *y* axis represents the ratio in MEP area between paired pulses and a single test pulse operation. In all cases the conditioning pulse amplitude was at 80% of MT, and the test pulse was at 120% of MT. Shown are means ± SE for 24 subjects.

Each point in the graph represents the mean and SE over 24 subjects for a certain ISI and capacitor combination.

As can be seen in Fig. 5, a cyclical pattern of relative inhibition and facilitation was observed. There is a clear facilitation at ISI = 0 (i.e., when the test pulse starts immediately at the end of the conditioning pulse). This is followed by a relative inhibition at an ISI of 400–600 μs, and a period of relative facilitation at 1–1.75 ms. At ISIs of 2.0–3.5 ms, some inhibition can be observed for certain capacitor combinations. There was a considerable degree of inter-subject variability in the locations of the ISI periods of inhibition and facilitation. Therefore, the observed minima and maxima in the averaged signal curve demonstrate the strength of this pattern.

Mixed model testing showed a significant effect for capacitor combination ($F = 8.494$, $P = 0.00014$) and ISI ($F = 11.468$, $P < 0.0001$) and also for the interaction term, (Capacitance × ISI) ($F = 1.497$, $P = 0.008$).

Note that with the experimental setup of this stage, using the *DCA*, after averaging overall subjects the strongest "inhibition" was actually a ratio of about 0.7–0.8. The 50/50 combination yielded on average the weakest inhibition.

The test pulse MEP areas obtained during the paired-pulses experiments are summarized in Table S1 in the Supplementary material. It can be seen that within-subject variability is much smaller than between-subject variability.

Selective inhibition using paired pulses

A significant inhibition was found for the paired pulses experiments with the conditioning pulse amplitude at 80% and test pulse amplitude at 120% of the *hand APB MT*, using the *4-Mod* Array. The results for ISIs of 200, 400 and 600 μs are shown in Fig. 6A for 27 subjects.
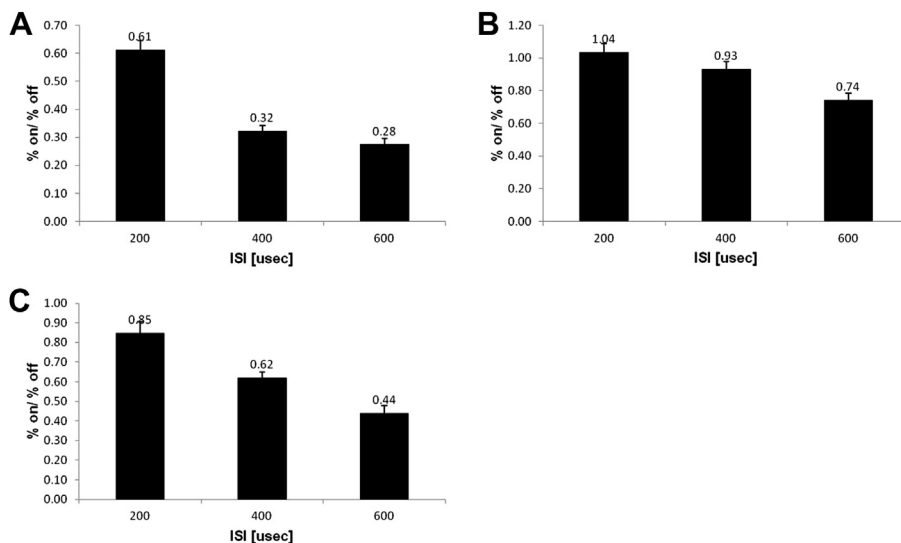

Figure 6. Excitability modulation induced by paired pulses at ISIs of 200, 400 and 600 μs, using the *4-Mod* Array. The *y* axis represents the ratio in MEP area between paired pulses and a single test pulse operation. A. For the hand APB muscle, with the conditioning pulse amplitude at 80% and the test pulse at 120% of the *hand APB MT*. Shown are means ± SE for 27 subjects. B. For the leg AH muscle, with the conditioning pulse amplitude at 80% of the *hand APB MT* and the test pulse at 120% of leg AH MT. Shown are means ± SE for 27 subjects. C. For the hand APB muscle, with the conditioning pulse amplitude at 80% of the *hand APB MT* and the test pulse at 120% of leg AH MT. Shown are means ± SE for 15 subjects.
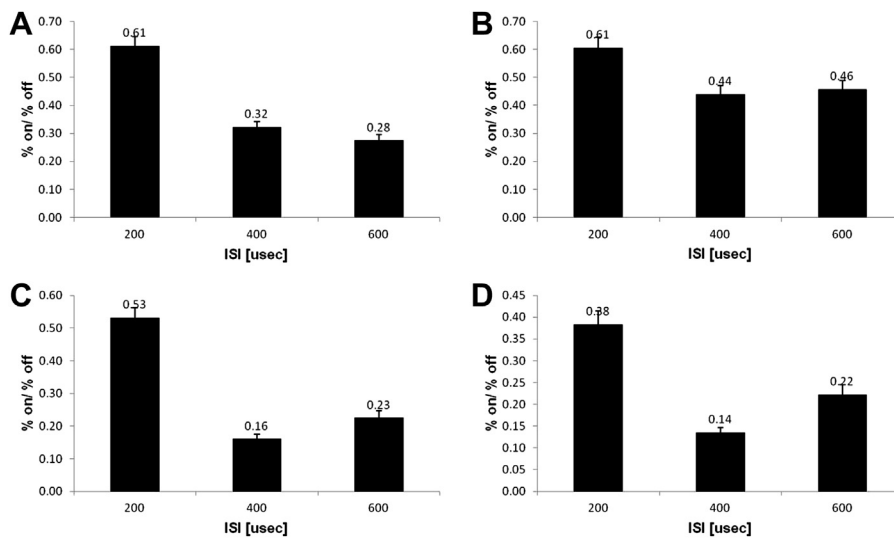
Figure 7. Excitability modulation induced by paired pulses at ISIs of 200, 400 and 600 μs, for the hand APB muscle using the *4-Mod* Array (A, n = 27), the leg AH muscle using the *4-Mod* Array (B, n = 27), the hand APB muscle using the *4-Mod 90°* Array (C, n = 21) and the leg AH muscle using the *4-Mod 90°* Array (D, n = 19). The y axis represents the ratio in MEP area between paired pulses and a single test pulse operation. In all cases the conditioning pulse amplitude was at 80% and the test pulse was at 120% of the relevant muscle MT.

The results for paired pulses applied over the leg motor cortex and measured at the leg AH muscle, with the conditioning pulse amplitude at 80% of the *hand APB MT* and the test pulse amplitude at 120% of the leg AH MT, are shown in Fig. 6B.

At any ISI, the difference in the paired pulses inhibition between the hand and the leg is significant ($P < 0.0001$, paired t-test). While for the leg there was almost no inhibition, for the hand there is a strong inhibition which peaks at ISIs of 400–600 μs.

The results for paired pulses applied over the hand motor cortex and measured at the hand APB muscle, with the conditioning pulse amplitude at 80% of the *hand APB MT* and the test pulse amplitude at 120% of the leg AH MT, are shown in Fig. 6C.

Effects of conditioning pulse orientation and motor cortex site on paired-pulse inhibition

The results of the paired pulses experiments measured at the hand APB and the leg AH muscles, with the *4-Mod* and the *4-Mod 90°* Arrays, are presented in Fig. 7. The number of subjects in each experiment is denoted at the figure legend.

The experiments results are summarized in Table 3.

Repeated measures 3-way mixed model revealed significant dependence on ISI ($P < 0.001$) and on orientation ($P < 0.001$), and significant limb × orientation interaction ($P = 0.016$). The limb × ISI interaction revealed a trend toward significance ($P = 0.083$).

In all cases average ratios of much less than 1 were found indicating strong inhibition. The maximal inhibition when using the *4-Mod 90°* Array occurred at ISI of 400 μs, while for the *4-Mod* Array over both the hand and the leg the results for ISIs of 400 and 600 μs were very similar.

Table 3
Excitability modulation results with paired pulses over hand APB and leg AH motor cortex.

Coil array	Muscle	ISI = 200 μs	ISI = 400 μs	ISI = 600 μs
4-Mod Array	Hand APB	0.61 ± 0.03	0.32 ± 0.02	0.28 ± 0.02
	Leg AH	0.61 ± 0.04	0.44 ± 0.03	0.46 ± 0.03
4-Mod 90° Array	Hand APB	0.53 ± 0.03	0.16 ± 0.01	0.23 ± 0.02
	Leg AH	0.38 ± 0.03	0.14 ± 0.01	0.22 ± 0.02

Interestingly the use of the *4-Mod 90°* Array where the orientation of the small coils pair inducing the conditioning pulse was at 90° to the larger coils pair inducing the test pulse resulted in significantly stronger inhibition.

The limb × orientation interaction term originated from the orientation dependence which was found to be stronger for the leg.

Simultaneous multi-channel operation of repetitive pulses

The operation parameters are described in Table 4.

The stimulator power output values used were at levels of about 120% of the average *hand APB MT* of each coil, as found in Section 3.2. All the trains were successfully produced as programmed. All output characteristics were produced in accord with the programmed parameters, with variability of 2.1%, 1.6% and 0.7% for the electric field amplitude, pulse width and inter-pulse interval.

Discussion

The novel Multiway multi-channel stimulator demonstrated simultaneous, sequential and repetitive operation of 2–5 channels, each operating a different coil, with variable stimulation parameters such as frequency and intensity.

This novel stimulator design opens the way for a broad range of clinical applications as well as neuroscience investigations. As a representative example, several imaging [33,34] and TMS [35] studies indicate that the role of the prefrontal cortex (PFC) in major depression disorder (MDD) is asymmetric, with relative hypo-activity in the left PFC, along with relative hyperactivity in the right PFC. This claim is supported by clinical data of several rTMS studies which found that MDD patient can benefit from antidepressant effect following excitatory high-frequency rTMS over the left PFC as well as following inhibitory low-frequency rTMS over the right PFC [36–38]. The multi-channel stimulator can be used to apply both rTMS treatment paradigms simultaneously and thus may enhance the clinical benefit. Similarly, other psychiatric and neurological diseases share multi-factorial nature, such that modulation of various components of the disease network will aid treatment efficiency.

Table 4
Operation parameters for multi-channel repetitive pulses experiments.

Coil array:		4 Ch Hand Array (4-HA)						
Channel	Capacitance [μF]	Coil	Power [%]	Frequency [Hz]	Train duration [s]	Inter-train interval [s]	No. of trains	Session length [min]
Protocol #1								
1	180	C	55	20	2	20	55	20.2
3	50	A	90	1	1200	–	1	20
4	50	B	90	5	4	16	70	23.3
5	180	D	55	10	4	20	55	22
Protocol #2								
1	180	C	55	20	2	20	80	29.3
3	50	A	90	1	2400	–	1	40
4	50	B	–	–	–	–	–	–
5	180	D	–	–	–	–	–	–

In addition, temporal combinations of differently shaped pulses can be combined to create complex pulse trains that can manipulate neuronal characteristics to enhance specific network effects. Even though the initial implementation of the stimulator used biphasic pulses, relatively simple modifications will allow the generation of monophasic pulses which can be combined in these pulse groups.

The integration of the rMT results and the phantom electric field measurements of two pairs of coils with very different dimensions and field decay profiles, yielded results of depths of stimulation sites which are in good agreement with previous studies reports regarding the hand [31,32,39] and leg [39] motor cortex. Previous studies [31,32,39] used identical capacitances and coils with similar inductances and obtained crossing points derived from plots of the electric field. In the case of this study the capacitances and inductances (hence the pulse widths) were very different for the two coil pairs. Therefore, the induced electric field intensities at the threshold of motor response were different. Yet the crossing points of the plots of the calculated change in trans-membrane potential yielded similar results for the hand and for the leg (Fig. S1 in the Supplementary material). The results of all the experiments (as summarized in Table 2) indicate that the critical change in the trans-membrane potential (V_m) required to induce motor response is fairly uniform over different cortical targets and coil characteristics. This finding is equivalent to the neural characteristics as reflected in the strength–duration curve [40].

The obtained values for V_m should not be taken as accurate estimations, but rather as comparative assessments of the variability in V_m in various experimental conditions.

The overall results indicate the well-known feature [4] that briefer TMS pulses produced by smaller capacitance circuits require less energy and have reduced heating rate even though they require higher capacitor voltages and currents to reach threshold. Simultaneous activation of four channels demonstrated reduction of 54% and 70% in energy consumption and heat dissipation, respectively, compared to a single channel operating a standard figure-8 coil. Comparison of channels with identical capacitors and similar coils found that doubling the number of channels operating simultaneously reduced the required energy consumption and heat dissipation by about 50%. This benefit results from the fact that when several coils are operated simultaneously via separate channels, the required capacitor voltage and coil current in each channel are substantially reduced. Note that the spatial and temporal characteristics of the induced electric field were different, and in general the field intensity induced by several coils using the same total energy consumption is higher compared to a single coil, and this contributed to the advantage of the multi-channel scheme. Comparison of single and multi-channel setups with identical field characteristics can be done by comparing several coils connected to separate channels, with the same coils connected in series to a single channel. In the latter case the total inductance, resistance and pulse width are higher, the electric field intensity required to reach threshold of neural stimulation is smaller, and calculations using Eqs. 14, 1 and 9 in the Supplementary material indicate that the multi-channel scheme is advantageous in energy consumption and heat dissipation.

These improved performance characteristics significantly extend the ranges of attainable stimulation intensity and/or frequency relative to currently available single-channel TMS stimulators and therefore expand the use of brain stimulation both in neuroscience and for clinical applications.

This study focused on the characteristics of the multi-channel stimulator compared to a single channel operation using the commonly-used biphasic pulses. It is reasonable to assume that combining the multi-channel device with other pulse shapes which were shown to improve efficacy [9–12] can lead to further reduction in energy requirements and coils heating rate. These promising possibilities should be addressed in future studies.

In the Pulse Group mode of the stimulator, the multi-channel stimulator demonstrated production of paired-pulses (or multiple pulses) with inter-pulse timings controlled at a resolution of 1 μs. The device enables for the first time to study paired-pulses effects with ISIs in the sub-millisecond regime. Using biphasic pulses with different capacitors combinations, a universal pattern was found independent of pulse width, with strong facilitation at ISI of 0 μs, followed by some inhibition which peaks at ISI of 400–600 μs. A strong facilitation was detected at ISIs of 1–1.5 ms, and another relative inhibition peak at ISIs of 2–2.25 ms. A dependence of the signal waveform on capacitor combination was found, and visually it was observed that the 180/50 and 180/180 combinations yielded stronger inhibition, while the 50/50 combination gave practically no inhibition. It therefore seems that the pulse width, especially of the conditioning pulse, has some effect on the neural response. The excitability modulation is probably dependent on the coils configurations and the exact neural populations affected by the conditioning and the test pulses. With the DCA, where the conditioning and the test pulses are produced by adjacent circular coils with very similar topology, position and orientation, the maximal relative inhibition gave a ratio of around 0.8, while for most other ISIs, various degrees of facilitation were observed. This can be contrasted to the 4-Mod and 4-Mod 90° Arrays, for which the conditioning and test pulses are produced by small and large figure-8 like configurations, respectively, a strong absolute inhibition was found for both the hand APB and the leg AH muscles for the ISIs that were employed (200–600 μs). This inhibition was orientation-dependent for both muscles, with a significantly stronger inhibition found for the 4 Mod 90 design (with conditioning coil pairs oriented at 90° to the test pulse coil pair). Moreover, this effect was stronger for the leg AH.

Interestingly, Ziemann and colleagues [30] found using monophasic pulses that the short interval intracortical inhibition (SICI)

induced with ISIs of 1–5 m at the hand abductor digiti minimi (ADM) was independent of the relative orientation of the conditioning and test coils. In contrast, for intracortical facilitation (ICF) at ISIs of 7–15 ms, the author found that the effect was dependent on the relative orientation of the coils. This result is partially in accord with our findings for inhibition at the hand APB where the orientation dependence was significant for ISI of 400 μs but not for ISIs of 200 and 600 μs. The cohort of the results seems to indicate that several mechanisms are involved in the excitability modulation processes. At ISI of 0 μs there is a residual effect of the first pulse on the transmembrane potential V_m, as can be seen in Fig. 2. In our scheme of a conditioning biphasic pulse of 80% of MT followed by a test biphasic pulse of 120% of MT, this residual effect leads to an increase of around 15% in the absolute value of the maximal V_m change in the first phase of the test pulse, which becomes similar to the maximal value in the second phase. Generally, when biphasic TMS pulses are used, at any specific neuronal site, depolarization occurs in one phase and hyperpolarization in the other [41], but the increased change in V_m in the first phase may lead to recruitment of additional neuronal sites which experience depolarization during the first phase. This mechanism may explain the significant facilitation shown at ISI of 0 μs. Obviously the use of different intensities of the conditioning pulse, or of different pulse shapes (such as monophasic) may lead to different results, and this must be investigated in future studies.

The apparent dependence on coils configurations suggests involvement of several mechanisms in the excitability modulations. For instance, there may be a universal inhibitory mechanism resulting from axonal refractoriness at ISIs <1 ms, in addition to facilitation induced by the residual effect of the first pulse. This facilitation may be stronger for configurations like the DCA where the conditioning and the test pulses are produced by coils with very similar topology and most probably affect similar neural populations. A similar mechanism may be responsible for the stronger inhibition found with the conditioning pulse orientation at 90° to the test pulse. The inhibition dependence on the conditioning pulse orientation was significantly stronger for the leg AH compared to the hand APB. This may result from differences in morphology and directional variability of the neural structures in the hand and leg motor cortex, or may suggest that different cortical inhibitory and facilitatory mechanisms are involved at the different motor sites. Indeed, several studies [42–46] point to the conclusion that the two peaks of inhibition observed with classical SICI experiments using monophasic pulses with figure-8 coils, at ISIs of 1 and 2.5 ms, result from different physiological mechanisms. The "early" inhibition at 1 ms is believed to be either a result of axonal refractoriness [43] or a synaptic process that differs to the one that causes the later inhibition [44,45]. Future studies with the Multiway using different pulse shapes including monophasic pulses with a control over the relative polarities of the conditioning and the test pulses may help to separate the various morphological, physiological and functional factors involved and unravel the underlying mechanisms.

When operating simultaneously several channels, one must take into account the magnetic coupling between coils which lead to mutual inductance and can affect the pulse shape and induced field intensity [15]. As was done in this study, overlapping coils should be connected to channels with identical capacitance to reduce interaction between channels.

The independent operation and temporal resolution of the various channels of the Multiway enables differential excitability modulation of different neuronal sites. This feature was demonstrated using conditioning and test pulses with ISIs of 400–600 μs produced by coils with different field decay profiles, and inducing strong inhibition at shallow cortical layer (hand motor cortex) and almost no inhibition at deeper region (leg motor cortex).

The ability to stimulate deeper neuronal structures using TMS was demonstrated in recent years using the deep TMS H-coils family [24–26], and has been found to provide promising potential benefit for the treatment of various brain disorders [47–51]. Operating the multi-channel stimulator with various TMS coils including H-coils in a spatially and temporally coordinated fashion may enable to increase the focality of deep TMS effect. Trains of such groups of paired pulses or multiple pulses can be applied in a repetitive TMS protocol, thus potentially enhancing the safety, efficacy and flexibility of the modality for a broad range of neurological and psychiatric disorders.

Acknowledgment

Appendix. Supplementary data

Supplementary data related to this article can be found at http://dx.doi.org/10.1016/j.brs.2013.09.004.

References

[1] Barker AT, Freeston IL, Jalinous R, Jarratt JA. Motor responses to non-invasive brain stimulation in clinical practice. Electroencephalogr Clin Neurophysiol 1985:S70.

[2] Barker AT, Jalinous R, Freeston IL. Non-invasive magnetic stimulation of human motor cortex. Lancet 1985;1:1106–7.

[3] Jalinous R. Principles of magnetic stimulator design. In: Pascual-Leone A, Davey K, Rothwell J, Wassermann EM, Puri BK, editors. Handbook of transcranial magnetic stimulation. London, UK: Arnold; 2002. pp. 30–8.

[4] Barker AT, Garnham CW, Freeston IL. Magnetic nerve stimulation: the effect of waveform on efficiency, determination of neural membrane time constants and the measurement of stimulator output. Electroencephalogr Clin Neurophysiol Suppl 1991;43:227–37.

[5] Hsu KH, Nagarajan SS, Durand DM. Analysis of efficiency of magnetic stimulation. IEEE Trans Biomed Eng 2003;50:1276–85.

[6] Ruohonen J, Virtanen J, Ilmoniemi RJ. Coil optimization for magnetic brain stimulation. Ann Biomed Eng 1997;25:840–9.

[7] MagVenture A/S. Product information sheet: MagPro X100 with option, technical data. DenMark: MagVenture; 2007. Available at: www.magventure.com.

[8] Magstim Bistim Manual. Available at: www.magstim.com; Magstim: UK.

[9] Goetz SM, Truong NC, Gerhofer MG, Peterchev AV, Herzog HG, Weyh T. Analysis and optimization of pulse dynamics for magnetic stimulation. PLos One 2013;8:e55771 [12 pp].

[10] Peterchev AV, Jalinous R, Lisanby SH. A transcranial magnetic stimulator inducing near rectangular pulses with controllable pulse width (cTMS). IEEE Trans Biomed Eng 2008;55:257–66.

[11] Peterchev AV, Murphy DL, Lisanby SH. Repetitive transcranial magnetic stimulator with controllable pulse parameters. J Neural Eng 2011;8:036016 [13 pp].

[12] Goetz SM, Pfaeffl M, Huber J, Singer M, Marquardt R, Weyh T. Circuit topology and control principle for a first magnetic stimulator with fully controllable waveform. Proc IEEE Eng Med Biol Soc 2012:4700–3.

[13] Ruohonen J, Ilmoniemi R. Focusing and targeting of magnetic brain stimulation using multiple coils. Med Biol Eng Comput 1998;36:297–301.

[14] Ruohonen J, Ravazzani P, Grandori F, Ilmoniemi RJ. Theory of multichannel magnetic stimulation: toward functional neuromuscular rehabilitation. IEEE Trans Biomed Eng 1999;46:646–51.

[15] Han BH, Chun IK, Lee SC, Lee SY. Multichannel magnetic stimulation system design considering mutual couplings among the stimulation coils. IEEE Trans Biomed Eng 2004;51:812–7.

[16] Wang X, Chen Y, Guo M, Wang M. Design of multi-channel brain magnetic stimulator and ANSYS simulation. IJBEM 2005;7:259–62.

[17] Im CH, Lee C. Computer-aided performance evaluation of a multichannel transcranial magnetic stimulation system. IEEE Trans Magn 2006;42:3803–8.

[18] Xu G, Chen Y, Yang S, Wang M, Yan W. The optimal design of magnetic coil in transcranial magnetic stimulation. Conf Proc IEEE Eng Med Biol Soc 2006;6:6221–4.

[19] Ho SL, Xu G, Fu WN, Yang QX, Hou HJ, Yan WL. Optimization of array magnetic coil design for functional magnetic stimulation based on improved genetic algorithm. IEEE Trans Magn 2009;45:4849–52.

[20] Lu M, Ueno S, Thorlin T, Persson M. Calculating the current density and electric field in human head by multichannel transcranial magnetic stimulation. IEEE Trans Magn 2009;45:1662–5.

[21] Yang S, Xu G, Wang L, Geng Y, Yu H, Yang Q. Circular coil array model for transcranial magnetic stimulation. IEEE Trans Appl Supercond 2010;20:829–33.

[22] Cao X, Cai D, Zhang X, Liu R, Tang J. Optimization of electric field distribution of multichannel transcranial magnetic stimulation based on genetic algorithm. BMEI 2010:1544–7.

[23] Deng Z-D, Peterchev AV. Transcranial magnetic stimulation coil with electronically switchable active and sham modes. IEEE Eng Med Biol Conf 2011:1993–6.

[24] Roth Y, Zangen A, Hallett M. A coil design for transcranial magnetic stimulation of deep brain regions. J Clin Neurophysiol 2002;19:361–70.

[25] Roth Y, Padberg F, Zangen A. Transcranial magnetic stimulation of deep brain regions: principles and methods. In: Marcolin M, Padberg F, editors. Transcranial stimulation as treatment in mental disorders. Advances in Biological Psychiatry, Vol. 23. Zurich, Switzerland: Karger Publishers; 2007. pp. 204–24.

[26] Zangen A, Roth Y, Voller B, Hallett M. Transcranial magnetic stimulation of deep brain regions: evidence for efficacy of the H-coil. Clin Neurophysiol 2005;116:775–9.

[27] Rossi S, Hallett M, Rossini PM, Pascual-Leone A. Safety, ethical considerations, and application guidelines for the use of transcranial magnetic stimulation in clinical practice and research. Clin Neurophysiol 2009;120:2008–39.

[28] Corthout E, Barker AT, Cowey A. Transcranial magnetic stimulation. Which part of the current waveform causes the stimulation? Exp Brain Res 2001;141:128–32.

[29] Kujirai T, Caramia MD, Rothwell JC, Day BL, Thompson PD, Ferbert A, et al. Corticocortical inhibition in human motor cortex. J Physiol 1993;471:501–19.

[30] Ziemann U, Rothwell JC, Ridding MC. Interaction between intracortical inhibition and facilitation in human motor cortex. J Physiol 1996;496(Pt 3):873–81.

[31] Epstein CM, Schwartzberg DG, Davey KR, Sudderth DB. Localizing the site of magnetic brain stimulation in man. Neurology 1990;49:666–70.

[32] Rudiak D, Marg E. Finding the depth of magnetic brain stimulation: a re-evaluation. Electroencephalogr Clin Neurophysiol 1994;93:358–71.

[33] Drevets WC. Neuroimaging studies of mood disorders. Biol Psychiatry 2000;48:813–29.

[34] Grimm S, Beck J, Schuepbach D, Hell D, Boesiger P, Bermpohl F, et al. Imbalance between left and right dorsolateral prefrontal cortex in major depression is linked to negative emotional judgment: an fMRI study in severe major depressive disorder. Biol Psychiatry 2008;63:369–76.

[35] Garcia-Toro M, Montes JM, Talavera JA. Functional cerebral asymmetry in affective disorders: new facts contributed by transcranial magnetic stimulation. J Affect Disord 2001;66:103–9.

[36] Burt T, Lisanby SH, Sackeim HA. Neuropsychiatric applications of transcranial magnetic stimulation: a meta analysis. Int J Neuropsychopharmacol 2002;5:73–103.

[37] Gershon AA, Dannon PN, Grunhaus L. Transcranial magnetic stimulation in the treatment of depression. Am J Psychiatry 2003;160:835–45.

[38] Levkovitz Y, Harel EV, Roth Y, Braw Y, Sheer A, Katz L, et al. Deep transcranial magnetic stimulation over the prefrontal cortex: evaluation of antidepressant and cognitive effects in depressive patients. Brain Stim 2009;2:188–200.

[39] Roth Y, Pell GS, Chistyakov AV, Sinai A, Zangen A, Zaaroor M. Motor cortex activation by H-coil and figure-8 coil at different depths. Combined motor threshold and electric field distribution study. Clin Neurophysiol 2013 Aug 29. http://dx.doi.org/10.1016/j.clinph.2013.07.013.

[40] Bourland JD, Nyenhuis JA, Noe WA, Schaefer JD, Foster KS, Geddes LA. Motor and sensory strength-duration curves for MRI gradient fields. New York: Proc Int Soc Magn Reson Med 4th Scientific Meeting and Exhibit; 1996. p. 1724.

[41] Pell GS, Roth Y, Zangen A. Modulation of cortical excitability induced by repetitive transcranial magnetic stimulation: influence of timing and geometrical parameters and underlying mechanisms. Prog Neurobiol 2011;93:59–98.

[42] Fisher RJ, Nakamura Y, Bestmann S, Rothwell JC, BostoCk H. Two phases of intracortical inhibition revealed by transcranial magnetic threshold tracking. Exp Brain Res 2002;143:240–8.

[43] Roshan I, Paradiso GO, Chen R. Two phases of short-interval intracortical inhibition. Exp Brain Res 2003;151:330–7.

[44] Hanajima R, Furubayashi T, Iwata NK, Shiio Y, Okabe S, Kanazawa I, et al. Further evidence to support different mechanisms underlying intracortical inhibition of the motor cortex. Exp Brain Res 2003;151:427–34.

[45] Vucic S, Cheah BC, Krishnan AV, Burke D, Kiernan MC. The effects of alterations in conditioning stimulus intensity on short interval intracortical inhibition. Brain Res 2009;1(1273):39–47.

[46] Cengiz B, Murase N, Rothwell JC. Opposite effects of weak transcranial direct current stimulation on different phases of short interval intracortical inhibition (SICI). Exp Brain Res 2013;225(3):321–31.

[47] Isserles M, Rosenberg O, Dannon P, Lerer B, Zangen A. Cognitive emotional reactivation during deep transcranial magnetic stimulation over the prefrontal cortex of depressive patients affects antidepressant outcomes. J Affect Disord 2011;128:235–42.

[48] Harel EV, Zangen A, Roth Y, Reti I, Braw Y, Levkovitz Y. H-coil repetitive transcranial magnetic stimulation for the treatment of bipolar depression: an add-on, safety and feasibility study. World J Biol Psychiatry 2011;12:119–26.

[49] Levkovitz Y, Rabany L, Harel EV, Zangen A. Deep transcranial magnetic stimulation add-on for treatment of negative symptoms and cognitive deficits of schizophrenia: a feasibility study. Int J Neuropsychopharmacol 2011;14:991–6.

[50] Onesti E, Gabriele M, Cambieri C, Ceccanti M, Raccah R, Di Stefano G, et al. H-coil repetitive transcranial magnetic stimulation for pain relief in patients with diabetic neuropathy. Eur J Pain 2013;17:1347–56.

[51] Isserles M, Shalev AY, Roth Y, Peri T, Kutz I, Zlotnick E, et al. Effectiveness of deep transcranial magnetic stimulation combined with a brief exposure procedure in post-traumatic stress disorder – a pilot study. Brain Stim 2013;6:377–83.